

# Synthesis and characterization of (Al, Co) co-doped ZnO for electronic applications

M. Ravindiran<sup>1</sup> · P. Shankar<sup>2</sup>

Received: 21 August 2016 / Accepted: 7 November 2016 / Published online: 17 November 2016  
© Springer Science+Business Media New York 2016

**Abstract** Synthesis of three different ratios of  $\text{Al}_{x=0.05, 0.10, 0.15} \text{Co}_{y=0.05, 0.10, 0.15} \text{ZnO}_{z=0.95, 0.90, 0.85}$  powders were prepared using sol gel route. Structural and electronic properties of the synthesized material were investigated using X-ray diffraction and scanning electron microscope, vibrating sample magnetometer (VSM), ultraviolet (UV) spectroscopy and dielectric studies. Characterization results reveal that the particle size is of the range 4.84 nm to the maximum size of 19.86 nm with a morphological structures representing rounded and honeycomb shapes at different doping ratios. VSM results of the prepared samples reveal the ferromagnetic nature with the hysteresis curve representation. The optical band gap has been calculated as 3.1–3.8 nm from the UV spectroscopy results. Conductivity of the samples was calculated from dielectric constant and conductivity increases with increasing doping ratios.

## 1 Introduction

Functional material synthesis and characterization are vital in matching novel materials for electronic applications, which significantly improve the device performance. The device performance can be further improved by the nano-materials and the nanostructures, which make the device

more suitable for various applications such as sensors, amplifiers and memory elements. Nanostructure and the nanomaterial's were fabricated with the sophisticated synthesis techniques and annealing temperatures. Nanobelts and nanorings of different sizes were synthesized with the Sn doped ZnO at the substrate temperatures of 700 and 800 °C and source materials temperature of 1000 °C. Synthesized nanobelts and nanorings have exhibited a change in the optical property with the band gap variation [1]. Device performance can be improved by modifying the device structures by introducing or replacing a material with enhanced property. Spintronic materials play a vital role in electronics which make the electron movement faster due to spin orientation. The spin orientation in magnetic material varies such as ferromagnetic, anti-ferromagnetic and diamagnetic depending on the nature of the material. Among the spintronic materials, ZnO is a promising material that has many applications in electronics. Pure ZnO has an improved electrical transport under visible light with respect to the variations in the impedance [2].

Similar to the binary compounds, ternary compounds also possess exciting properties when synthesized for various electronic applications. Some of the ternary compounds are AlGaSb, AlGaAs, GaInAs, AlInAs, GaInSb, AlInSb, InAsSb, GaAsSb, GaInP, AlInP, AlGaP, GaAsP, InAsP and InMnSb. Fe and Cu doped ZnO compounds synthesized by wet chemical route exhibit a good ferromagnetic nature [3]. Analysis based on first principle calculations is an easy route to analyze the electronic and magnetic properties of the ternary compounds. Co and Al doped ZnO ternary compound has been analyzed by various first principle study routes such as Ruderman–Kittel–Kasuya–Yosida (RKKY) interaction and Ab initio density-functional calculations [4, 5]. Co and Al doped ZnO Nano

✉ M. Ravindiran  
ravmun@gmail.com

<sup>1</sup> Department of Electronics and Communication, Saveetha School of Engineering, Saveetha University, Thandalam, Chennai, India

<sup>2</sup> Amrita School of Engineering, Amrita University, Vengal Village, Chennai, India

**Table 1** Sample composition and doping ratios

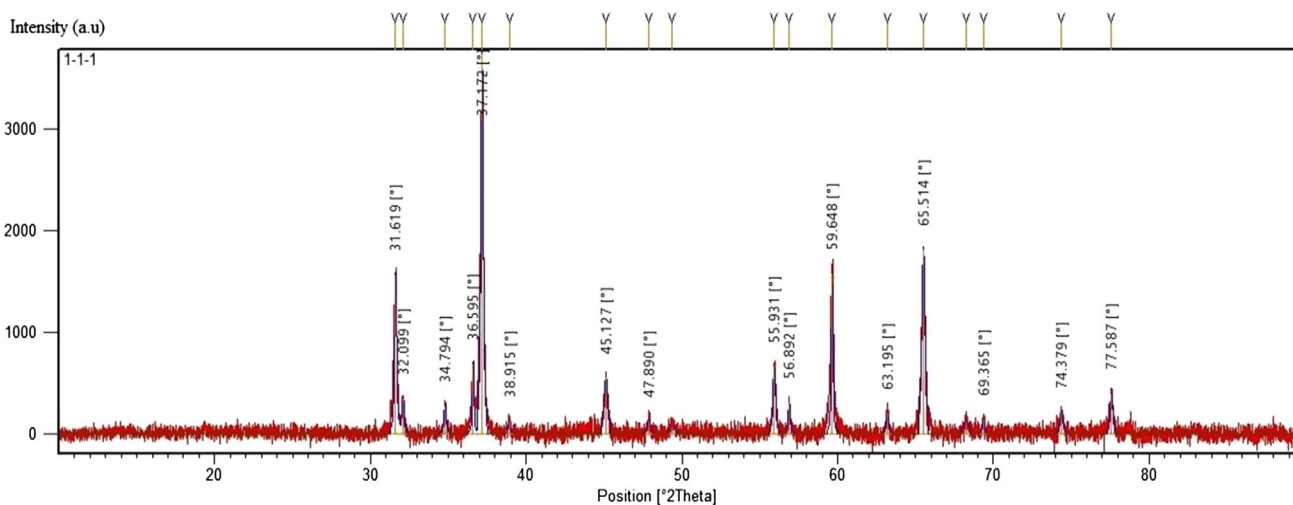
Sl. no	Sample	Ratio		
		(Zn (CH <sub>3</sub> COO) <sub>2</sub> )	Co(NO <sub>3</sub> ) <sub>2</sub>	Al(NO <sub>3</sub> ) <sub>3</sub>
1	A	0.95	0.05	0.05
2	B	0.90	0.10	0.10
3	C	0.85	0.15	0.15

powders and thin films of various doping ratios such as Zn<sub>0.95-x</sub>Co<sub>0.05</sub>Al<sub>x</sub>O ( $x = 0.0-0.1$ ), Zn<sub>0.85</sub>Co<sub>0.10</sub>Al<sub>0.05</sub>O, Zn<sub>0.94</sub>Co<sub>0.05</sub>Al<sub>0.01</sub>O and Zn<sub>0.95-x</sub>Co<sub>0.05</sub>Al<sub>x</sub>O ( $x = 0, 0.01, 0.03$ ) has ferromagnetic behavior at various temperatures. Some samples show ferromagnetism at room temperature while some samples exhibit ferromagnetism at higher temperatures. Most of the samples reveal improved ferromagnetism with increased concentration of Al in ZnO lattice. In some samples ferromagnetism is observed at 360 K and the ternary compound very well suits the Dilute Magnetic Semiconductor application in electronics [6–9].

Doped and undoped ZnO has many applications such as Microelectronic devices, Sensors, UV lasers, Thin Film Transistors (TFT), High electron mobility transistor (HEMT), Flexible memories, Light emitting diodes, Diodes, Photo detectors, Field emitters, Surge arresters and Photovoltaic devices. The property of the material and the application varies with the fabrication process, structure, synthesis methods, doped material and doping concentrations. In the form of thin film, ZnO can be used as TFT and HEMT and higher mobility for flexible electronic applications such as displays [10]. Nanostructured and nanowire ZnO can be used in Transistor, Phototransistor and Photovoltaic energy conversion device applications. ZnO nanowire transistor shows a field effect mobility of 928 cm<sup>2</sup>/Vs, which will enable the transistors to achieve

the higher performances [11]. As similar to the above application, ZnO can be made into high electron mobility nanocomposite TFT by dispersing an array of nanostructures in n- and p-type organic semiconductor host matrices. Performance enhancement with device mobility of 0.3–0.6 cm<sup>2</sup> V<sup>-1</sup>s<sup>-1</sup> and on–off ratios as 10<sup>6</sup>, are reported [12]. Another application of ZnO is high-response photo detector, when used as a gate oxide in the metal oxide semiconductor field effect transistor. The photo response recorded in the device is around 1500 A/W under white light illumination, which is very high when compared to the other detectors [13].

ZnO based sensors have been used in various sensing applications such as pH sensing, humidity Sensing and acetone sensing. Al doped ZnO nanostructures have improved sensitivity when used as extended gate field effect transistor. The sensitivity of the device with the Al doped nanostructure extended gate FET has an improved sensitivity of 57.95 mV/pH [14]. ZnO coated over porous silicon has an improved humidity sensing with the varying electrical conductivity, the response time varies with the change in humidity [15]. Thin films made of In doped ZnO exhibit good acetone sensing ability. In the case of In-doped ZnO films, almost 96.8% sensing was achieved for the 100 ppm of acetone in air at room temperature. The sensing response of the sensor was reported to be improved with the increasing temperature [16]. Besides the sensor application, ZnO is used as lasers and flexible memories. When ZnO is embedded into SiO<sub>2</sub>, it works as Ultraviolet lasers with lasing around 388 nm [17]. ZnO-based flexible memories were fabricated using sol gel process by metal insulator metal structure with resistive switching characteristics. Prepared films had demonstrated a fast programming of less than 50 ns and high off to on resistance ratio of greater than 10<sup>4</sup> [18].

**Fig. 1** XRD pattern of CoAl doped ZnO with the material composition Al<sub>x=0.05</sub> Co<sub>x=0.05</sub> ZnO<sub>x=0.95</sub>

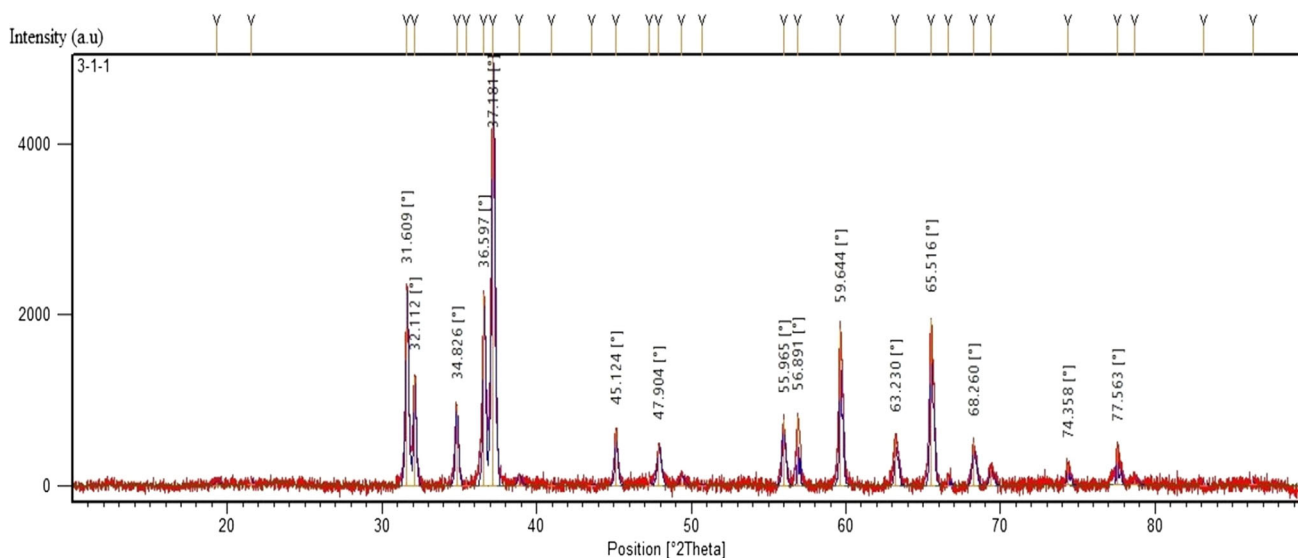


**Fig. 2** XRD pattern of CoAl doped ZnO with the material composition  $\text{Al}_{x=0.10} \text{Co}_{x=0.10} \text{ZnO}_{x=0.90}$

Diodes and LEDs are fabricated using ZnO and doped ZnO as part of the layer in the device structures. Ga doped ZnO exhibits blue light emitting application with the output power of 1.6 mW at the current of 35 mA when used as top contact [19]. Increased current injection and red shifted property for color tunable and spin LED effect have been observed in the Fe doped ZnO Nanorod arrays on the *P* type Si substrates [20]. Schottky diode characteristics were observed in Mn doped ZnO thin films. The pure and Mn doped ZnO films sandwiched between pt electrodes exhibit a schottky barrier at Pt/Mn doped ZnO interface [21].

The power conversion efficiency of the Photovoltaic (PV) devices is improved with various nanomaterials and nanostructures. ZnO is one among the most promising materials to be used for photovoltaic applications. Organic PV devices can be fabricated by the flexible and transparent single walled CNT's when used as a substrate and ZnO nanowires grown over it. The power conversion efficiency of the device is calculated to be around 0.6%, which confirms that the device will be a promising optoelectronic and energy harvesting candidate [22]. Improved power conversion efficiency of 12.5% and exceedingly high electrical and optical properties are achieved in Al doped ZnO thin film solar cell [23]. Dye-sensitized solar cells are increasingly popular due to the improved performance. Dye-sensitized solar cell with energy storage function was fabricated through PVDF/ZnO nanocomposite counter electrodes. Energy conversion efficiency of 3.7% and energy storage capability of  $2.14 \text{ Cg}^{-1}$  were achieved with the mentioned structure [24]. MgO and rGO doped ZnO nanoparticles exhibit better photocatalytic, photovoltaic and photo detection properties at natural sun irradiation to be matched for various optoelectronic

applications [25]. Improved photocurrent was observed with the cadmium oxide (CdO) and reduced carbon oxide (rGO) doped ZnO nanoparticles. Observed photocurrents for ZnO, ZnCdO and ZnCdOrGO are 15, 43 and  $47 \mu\text{A Cm}^{-2}$ . Similarly alkaline metals doped ZnO nanoparticles exhibit better photocurrent under visible illumination with varying doping concentrations. The photocurrent of the ZnO, Li doped ZnO, Na doped ZnO and K doped ZnO exhibits the photocurrent of 6.3, 6.7, 6.8 and  $8 \mu\text{A Cm}^{-2}$ , which will make the alkaline doped ZnO nanoparticles more suitable for a high sensitive visible light photo detectors [26, 27].

## 2 Experimental

Zinc acetate was dissolved in distilled water to make a solution of concentration 10 M and stirred in magnetic stirrer for 10 min. Cobalt nitrate was dissolved in distilled water to obtain a solution of concentration 4 M and mixed with the Zinc acetate. Finally Aluminum Nitrate was dissolved in distilled water of 4 M and stirred, then dissolved with the Co:ZnO solution in the magnetic stirrer. The resulting solution was allowed to be stirred in the magnetic stirrer for 40 min with a temperature of 60 °C. After the continuous stirring of the solution a homogenous mixture of gel is formed. The gel is kept in the hot air oven at 100 °C for 24 h and then dried up at the atmospheric temperature. Then the dried powder was annealed at 750 °C for 4 h to get the green colored powders. The doping concentration of the compound was varied for three different ratios such as  $x=0.05, 0.10, 0.15$   $\text{Co}_{x=0.05, 0.10, 0.15} \text{ZnO}_{x=0.95, 0.90, 0.85}$  (Table 1).

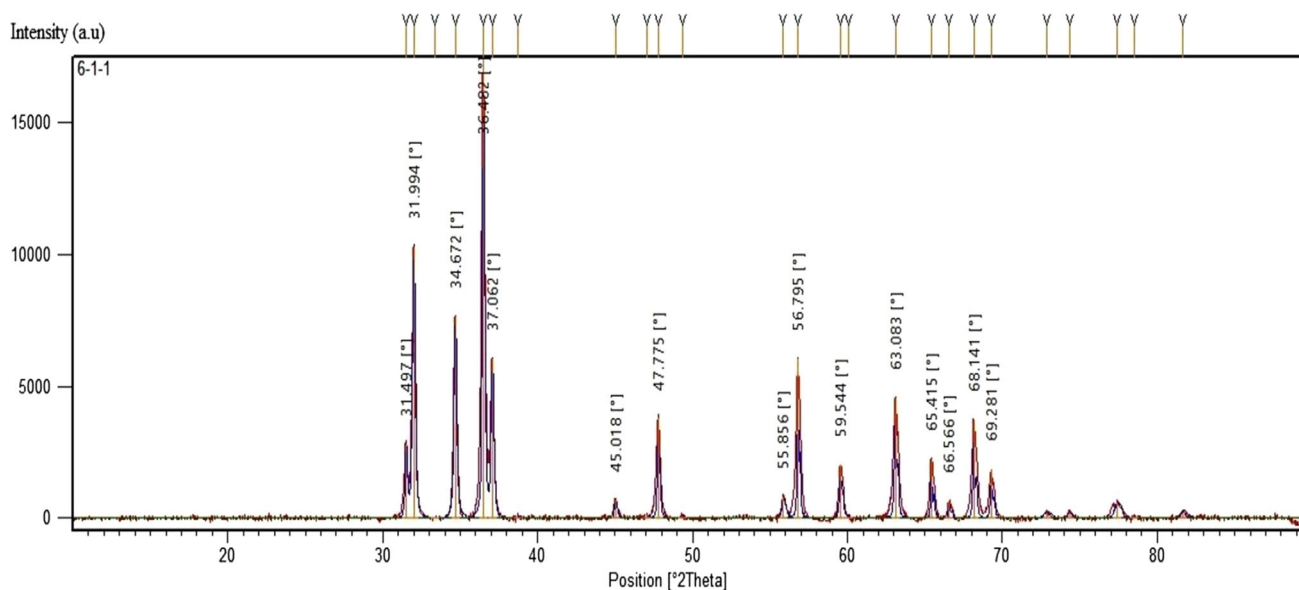


**Fig. 3** XRD pattern of CoAl doped ZnO with the material composition  $Al_{x=0.15} Co_{x=0.15} ZnO_{x=0.85}$

**Table 2** Sample A XRD parameters

Pos. (°2Th.)	Height (cts)	FWHM (°2Th.)	D-spacing (Å)	Rel. int. (%)	Particle size (nm)
31.6189	1568.57	0.1728	2.82741	41.95	8.25
32.0986	344.64	0.1920	2.78625	9.22	7.44
34.7942	279.73	0.1920	2.57631	7.48	7.48
36.5952	692.80	0.1344	2.45355	18.53	10.79
37.1715	3739.01	0.1920	2.41682	100.00	7.53
45.1267	561.65	0.3072	2.00753	15.02	4.84
47.8899	129.79	0.2688	1.89795	3.47	5.59
55.9305	663.09	0.1920	1.64265	17.73	8.11
56.8923	310.38	0.1536	1.61715	8.30	18.03

Zinc acetate ratio was varied of different proportions', whereas the Cobalt nitrate and Aluminium nitrate was kept constant with the same ratios for each sample.

### 3 Results and discussion

Material characterizations such as X-ray Diffraction (XRD), scanning electron microscopy (SEM), ultraviolet spectroscopy (UV), dielectric and vibrating sample magnetometer (VSM) were done to analyze the structural, optical, electrical and magnetic property of the synthesized materials.

#### 3.1 XRD spectroscopy

XRD analysis confirms the material presence in the compound with the reference to the JCPDS and literatures. Particle size can also be analyzed with the help of the Scherer equation as mentioned below.

$$S = \frac{K\lambda}{\beta \cos\theta} \quad (1)$$

$K$ —0.89,  $\lambda$ —X ray Wavelength,  $\beta$ —full width half maximum,  $\theta$ —Bragg's angle

XRD analysis of the three samples was done with the JCPDS data base reference to identify the presence and phase of the particles in the synthesized compounds. Particle size was calculated with the Scherrer equation. Corresponding Figs. 1, 2 and 3 give the X-ray peaks at various  $2\theta$  angles and their intensities. Comparison with the JCPDS data base gives the presence of the Al, Co and ZnO at different planes. The peaks at the  $2\theta$  angles  $32^\circ$ ,  $34^\circ$  and  $36^\circ$  with the hkl planes 100, 002 and 101 conforms the presence of the ZnO. Similarly the peaks at  $31^\circ$ ,  $37^\circ$ ,  $45^\circ$ ,  $47^\circ$ ,  $48^\circ$  and  $55^\circ$  represents the peaks of Al and Co doped ZnO. The above materials identification is done with reference to the JCPDS database (36-1451) and (34-1470) respectively. Particle size of the three samples has been calculated and the size remains smallest of 4.84 nm to the

**Table 3** Sample B XRD parameters

Pos. (°2Th.)	Height (cts)	FWHM (°2Th.)	D-spacing (Å)	Rel. int. (%)	Particle size (nm)
32.1118	1273.17	0.1574	2.78745	25.54	9.07
34.8265	941.32	0.1889	2.57613	18.88	7.60
36.5967	2242.55	0.1732	2.45549	44.99	8.38
37.1806	4985.09	0.2204	2.41826	100.00	6.58
45.1238	645.25	0.1574	2.00932	12.94	9.45
47.2974	99.45	0.0787	1.92192	1.99	19.03
47.9044	471.37	0.2519	1.89898	9.46	5.95
55.9654	779.53	0.1889	1.64307	15.64	8.25
56.8905	809.37	0.0787	1.61853	16.24	19.86

**Table 4** Sample C XRD parameters

Pos. (°2Th.)	Height (cts)	FWHM (°2Th.)	D-spacing (Å)	Rel. int. (%)	Particle size (nm)
31.4968	2835.73	0.1506	2.84045	16.21	9.51
31.9935	10283.74	0.2007	2.79748	58.80	7.13
34.6718	7637.07	0.2007	2.58727	43.67	7.17
36.4817	17489.55	0.1506	2.46296	100.00	9.58
37.0622	6058.39	0.1840	2.42571	34.64	7.87
45.0178	754.36	0.1673	2.01380	4.31	8.9
47.0589	156.87	0.1004	1.93110	0.90	14.89
47.7746	3796.09	0.1338	1.90384	21.70	11.23
55.8557	849.11	0.2342	1.64604	4.85	6.62
56.7947	6060.01	0.1171	1.62103	34.65	13.30
66.5665	675.43	0.1338	1.40482	3.86	12.34

maximum size of 19.86 nm. Average particle size absorbed in the three samples is around 7–9 nm (Table 2, 3 4).

**3.2 SEM analysis**

SEM images (Fig. 4) reveal the different structural morphology of the three different samples at varying magnifications of 100.00, 200.00 and 500.00 K. The SEM micrographs of the three samples are annealed with 750 °C and the structural morphology of the samples reveals the rounded shapes in sample 100.00 K magnification of sample A and 200.00 K magnification of Sample B. Similarly the Sample B by 100.00 K magnification and sample C with 200.00 K magnification are also showing rounded shaped. Honeycomb structure is resembled with the sample A image of 200.00 and 500.00 K magnification.

**3.3 VSM**

VSM graphs with M–H curves of the three samples are shown in the Fig. 5. Hysteresis curves of the samples vary with the doping ratios. Thin ferromagnetic nature is established in the M–H curves of the three samples, whereas the sample C of the material composition  $Al_{x=0.15}$

$Co_{x=0.15}ZnO_{x=0.85}$  is having a better hysteresis curve when compared to the other two samples. The better hysteresis curve for the representation of the ferromagnetism is due to the doping ratios of the AlCoZnO compound. The increasing dopant ratios of the Al and Co results in the improvement in the hysteresis curve. A better hysteresis curve can be established by the change in the magnetic moment, field and temperature range of the VSM settings.

**3.4 UV spectroscopy**

Figure 6 shows the optical absorption spectrum of the AlCo doped ZnO material with three different compositions named as A, B and C respectively. All the three absorption spectra results have the peaks almost at 350 nm, which implies that all the three samples have the smaller particle size. Optical band gap of the samples was calculated from the Eq. 2. Calculated optical band gap from the UV cut off at 325–400 nm is 3.82–3.10 eV. The optical band gap reveals that the increasing doping concentrations make the band gap smaller. Optical property and the size of the material can be more clearly understood by the UV spectroscopy [28–30] (Table 5).

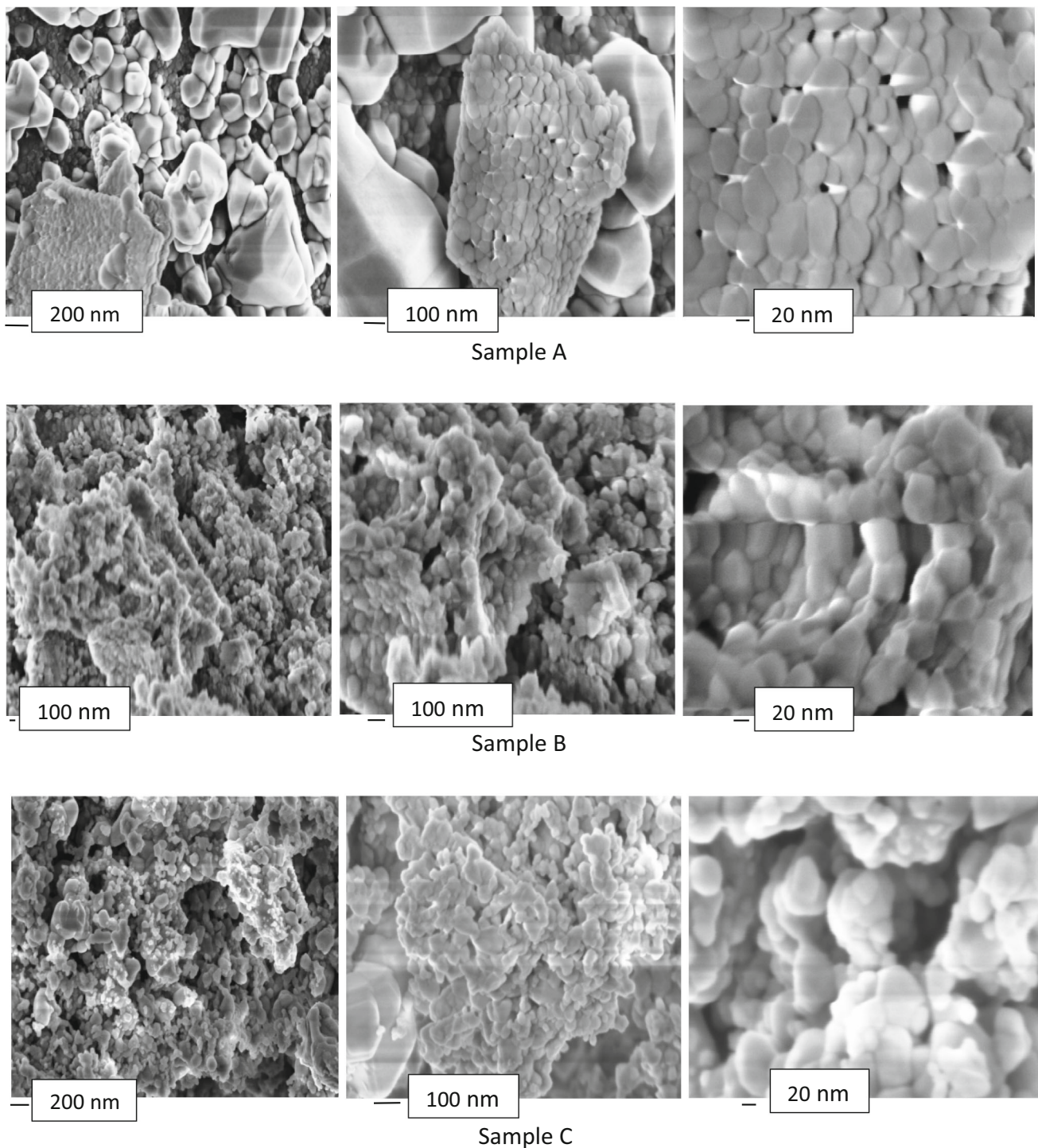


**Fig. 4** SEM images of samples A, B and C at 100.00, 200.00 and 500.00 K magnifications

$$E = \frac{hc}{\lambda} \quad (2)$$

where  $h$  = Planck's constant =  $6.626 \times 10^{-34}$  J sec,  $c$  = Speed of Light =  $3.0 \times 10^8$  m/sec,  $\lambda$  = cut off wavelength = for samples A and B 325 nm, for sample C 400 nm

### 3.5 Dielectric properties

Dielectric properties of the synthesized materials have been done by pelletizing the material with the thickness of 1 mm. Properties such as dielectric constant, loss function

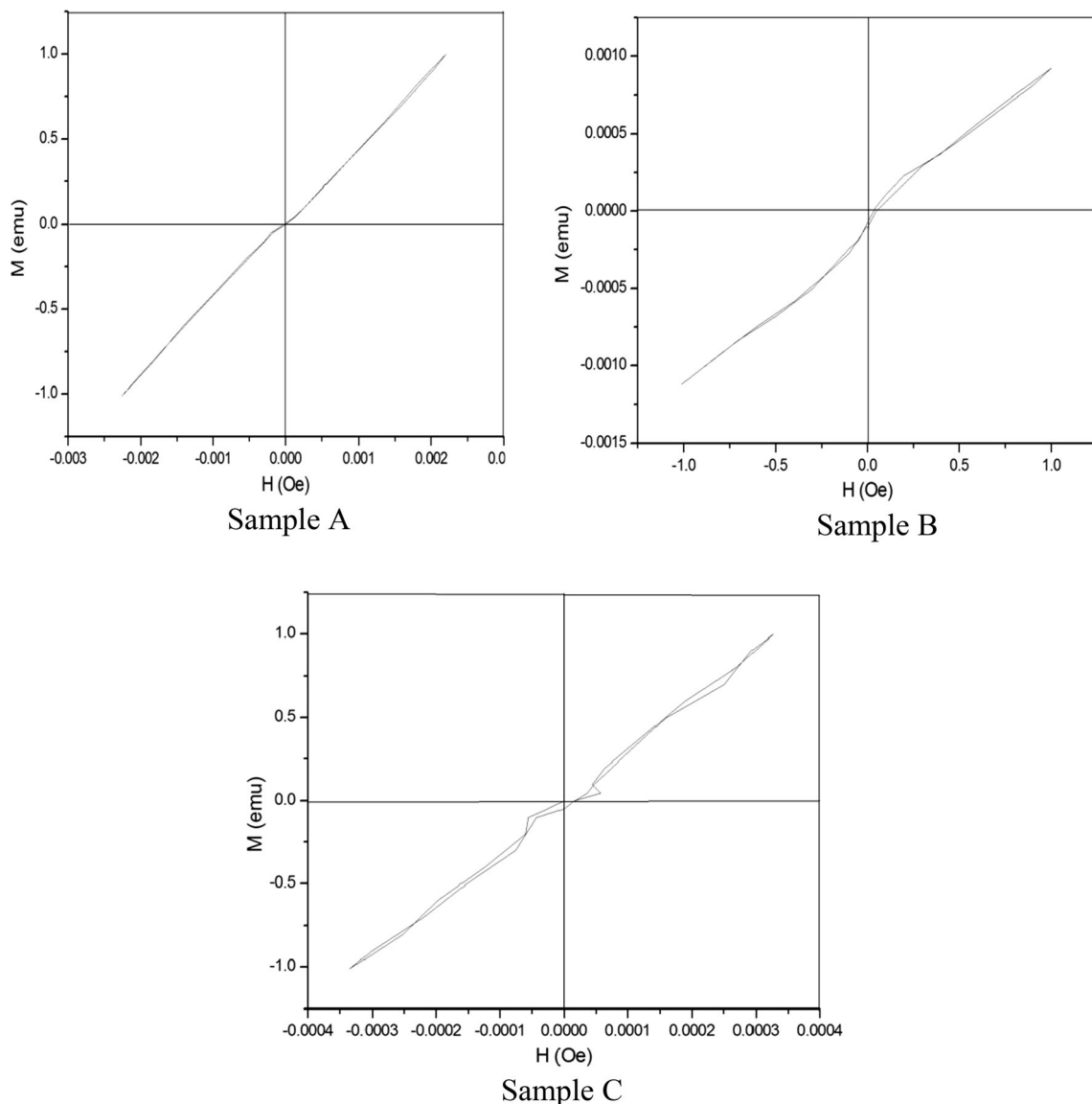


Fig. 5 VSM Graphs of samples A, B and C

and conductivity have been done with the Eqs. (3), (4) and (5) [31, 32] (Fig. 7).

$$\frac{tXCp}{\pi(\frac{d}{2})^2 X \epsilon_0} \tag{3}$$

$$D = \frac{\epsilon i}{\epsilon r} \tag{4}$$

$$\frac{2\pi f C p D t}{A} \text{ (S/m)} \tag{5}$$

t = thickness of the pellet, Cp = parallel capacitance, d = diameter of the guard electrode =  $5 \times 10^{-3}$ (m),  $\epsilon_0$  = permittivity of vacuum =  $80,854 \times 10^{-12}$  (F/m),  $\epsilon_i$  = dielectric loss,  $\epsilon_r$  = dielectric constant, f = frequency, D = dissipation factor, A = area of the electrode

Figure 7a gives the dielectric constant of the samples A, B and C with the varying frequency range from 0 to 1,000,000 Hz. It is evident from the graph that the dielectric constant of the sample C is very high at the low frequency and linearly decreases with the increasing frequency similar to the ZnO loaded ortho-chloropolyanilin-nano composite as reported by Aashish Roy [33]. Figure 7b describes the dielectric loss of the three samples, where the loss linearly decreases with the increasing frequencies. Conductivity plots of the samples A, B and C has been explained in the Fig. 7c. The conductivity improves with the doping concentrations of the samples with respect to the frequency. Sample C with the doping concentrations of Al<sub>x=0.05</sub> Co<sub>x=0...</sub>05ZnO<sub>x=0.95</sub> has an improved conductivity when compared to the other two samples.

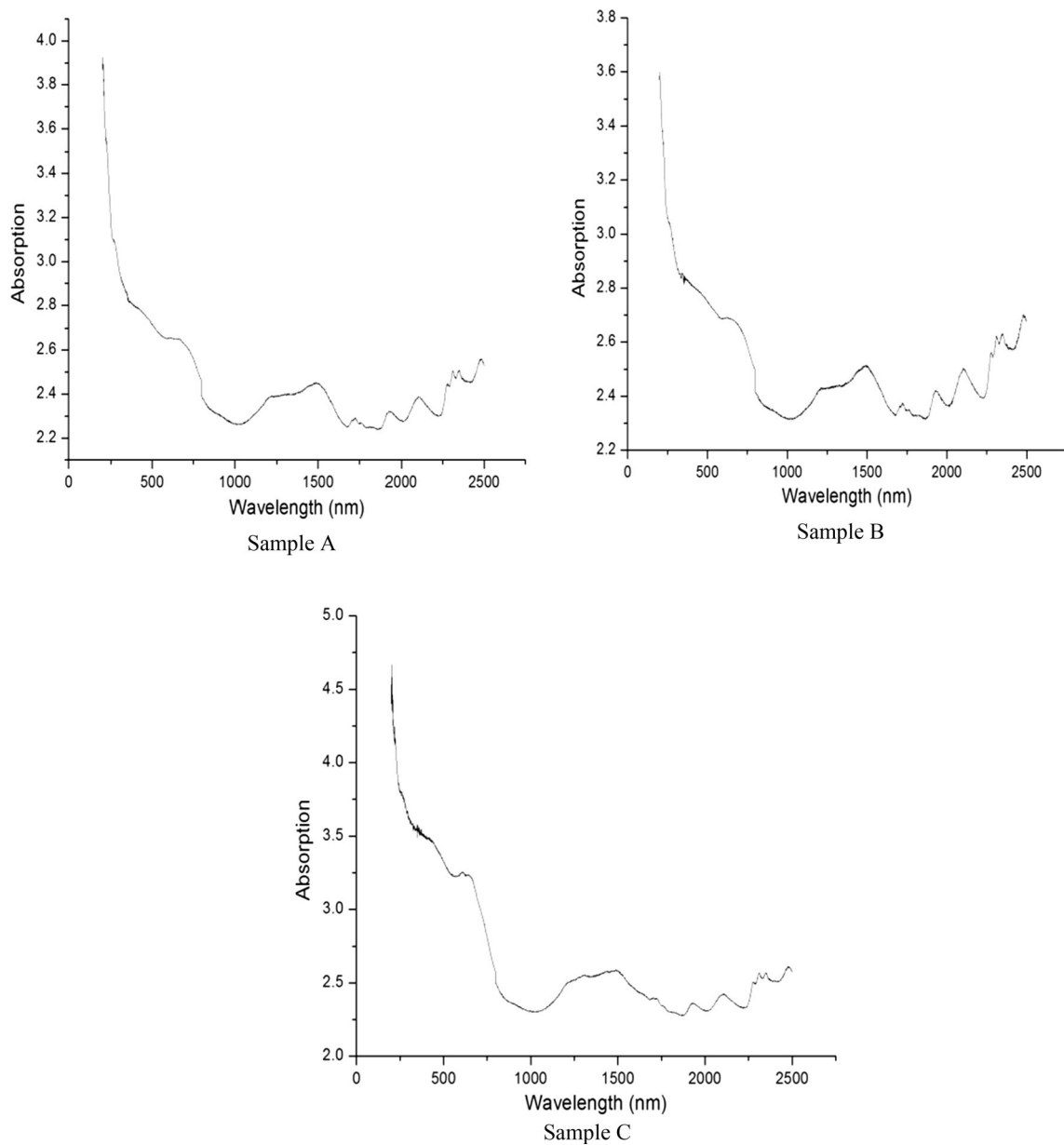


**Fig. 6** UV absorption spectra of samples **A**, **B** and **C**

**Table 5** Optical band gap

Sl.No	Samples	h	c	$\lambda$	E	eV
1	A	$6.626 \times 10^{-34}$	$3.0 \times 10^8$	325	$6.116 \times 10^{-33}$	3.822
2	B	$6.626 \times 10^{-34}$	$3.0 \times 10^8$	325	$6.116 \times 10^{-33}$	3.822
3	C	$6.626 \times 10^{-34}$	$3.0 \times 10^8$	400	$4.969 \times 10^{-33}$	3.10

$$1 \text{ eV} = 1.6 \times 10^{-19} \text{ J}$$



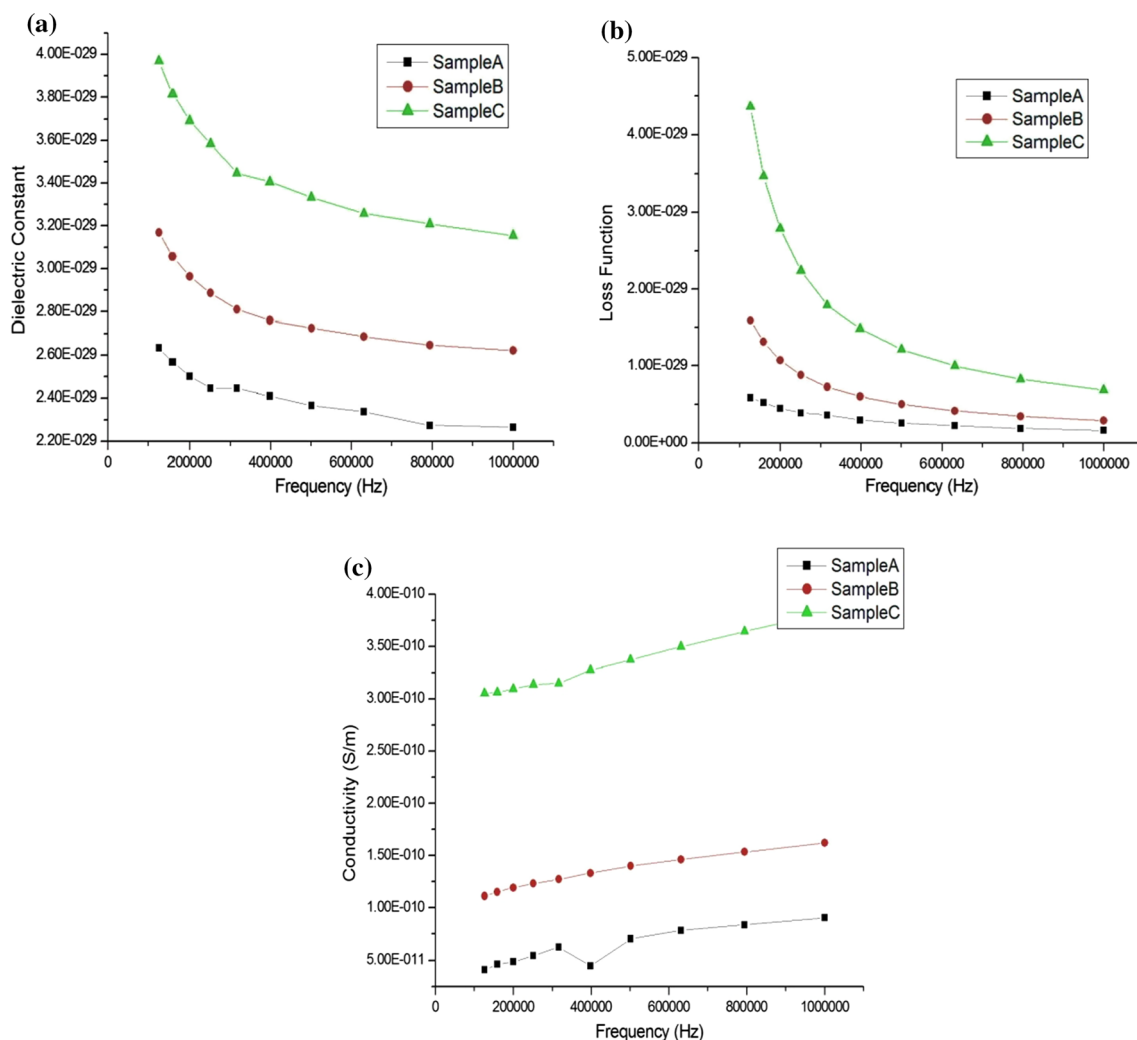


**Fig. 7** Dielectric properties: **a** dielectric constant, **b** loss function and **c** conductivity of *samples A, B and C*

## 4 Conclusion

Doping ratios with the same concentration of Al and Co into ZnO has revealed a very good structural, electronic, optoelectronic and magnetic property. Ternary compound has improved property with the ratios of  $\text{Al}_{x=0.15} \text{Co}_{x=0.15} \text{ZnO}_{x=0.85}$ . UV spectroscopy result reveals that the particle size is small with the optical band gap of 3.82–3.10 eV. The band gap has diminished with the increased doping concentrations of the Al and Co. Similar to the UV spectroscopy; conductivity analysis based on the dielectric studies reveals an improved conductivity with the increasing doping concentrations of the dopants. Hysteresis loop of the samples reveals that the material to be ferromagnetic, which will support the spintronic based device applications.

**Acknowledgements** The authors thank the Management of Saveetha University for the continuous motivation to carry out the research

work and for extending all necessary support. We would also like to extend our regards to Sophisticated Analytical Instruments Facility (SAIF), IIT Madras and Indira Gandhi Centre for Atomic Research (IGCAR) for carrying out the material characterizations.

## References

1. R. Yousefi, Effects of Sn atoms on formation of ZnO nanorings. *Cryst. Eng. Comm.* **17**, 2698 (2015)
2. S. Dusari, J. Barzola-Qaiquia, P. Esquinazi, Changes in the electrical transport of ZnO under visible light. *Solid State Commun.* **150**, 22–26 (2010)
3. O.D. Jayakumar, I.K. Gopalakrishnan, S.K. Kulshreshtha, Magnetization study of Fe doped ZnO co-doped with Cu: synthesised by wet chemical method. *J. Mater. Sci.* **41**, 4706–4712 (2006)
4. T. Zhang, L.X. Song, H.W. Zhang, Origin of ferromagnetism of (Co, Al) codoped ZnO from first principle calculations. *App. Phys. Lett.* **89**, 172502 (2006)
5. D. Iusan, R. Knit, B. Sanyal, O. Eriksson, Electronic structure and chemical and magnetic interactions in ZnO doped with Co and Al: experiments and ab initio density-functional calculations. *Phys. Rev. B* **78**, 085319 (2008)

6. O.D. Jayakumar, S.N. Achary, C. Sudakar, A.K. Tyagi, Experimental and Theoretical investigation on magnetic behaviour of (Al, Co) co-doped ZnO nanoparticles. *Nanoscale* **2**, 1505–1511 (2010)
7. C.S. Chang, E.Z. Kurmaev, A. Dinia, Co and Al co-doping for ferromagnetism in ZnO: co diluted magnetic semiconductors. *J. Phys. Cond. Matter* **21**, 056002 (2009)
8. M. Sharma, R.M. Mehra, Effect of thickness on structural, electrical, optical and magnetic properties of Co and Al doped ZnO films deposited by sol–gel route, *App. Surf. Sci.* **255**, 2527–2532 (2008)
9. X.C. Liu, E.W. Shi, L.X. Song, High temperature ferromagnetism in (Co, Al) codoped ZnO powders. *App. Phys. Lett.* **88**, 252503 (2006)
10. H.E. Unalan, Y. Zhang, P. Hiralal, G.A.J. Amaratunga, Zinc oxide nanowire networks for macroelectronic devices. *App. Phys. Lett.* **94**, 163501 (2009)
11. H.E. Unalan, Y. Yang, Y. Zhang, P. Hiralal, G. Amaratunga, ZnO nanowire and WS<sub>2</sub> nanotube electronics. *IEEE Trans. Electron. Device* **55**, 2988–3000 (2008)
12. Flora M. Li, Gen-Wen Hsieh, William I. Milne, Zinc oxide nanostructures and high electron mobility nanocomposite thin film transistors. *IEEE Trans Electron. Device* **55**, 3001–3011 (2008)
13. E. Lee, D.I. Moon, Y.K. Choi, Transparent zinc oxide gate metal oxide-semiconductor field effect transistor for high responsivity photodetector. *IEEE Electron. Device Lett.* **30**, 493–495 (2009)
14. J.L. Wang, P.Y. Yang, M.H. Juang, pH sensing characteristics of Hydrothermal Al–doped ZnO nanostructures, *J. Nano. Mat.* **2013**, 1–7 (2013)
15. Jiang T., Zhou X. and Luo T., A zinc oxide modified porous silicon humidity sensor, *Proceeding of the IEEE International Conference on Information Acquisition*, (2006)
16. C.S. Prajapati, P.P. Sahay, Influence in doping on the structural, optical and acetone sensing properties of ZnO nanoparticulate thin films. *Mat. Sci. Semicond. Process.* **16**, 200–210 (2012)
17. E.S.P. Leong, M.K. Ching, S.F. Yu, Sol–Gel ZnO–SiO<sub>2</sub> composite waveguide Ultraviolet Lasers. *IEEE Photon. Technol. Lett.* **16**, 2418–2420 (2004)
18. S. Kim, H. Moon, D. Gupta, Y.K. Choi, Resistive switching characteristics of Sol–Gel zinc oxide films for flexible memory applications. *IEEE Trans. Elect. Device* **56**, 696–699 (2009)
19. C.L. Liao, Y.F. Chang, M.C. Wu, High speed GaN based blue light emitting diodes with gallium DOPED ZnO current spreading layer. *IEEE Elect. Dev. Lett.* **34**, 611–613 (2013)
20. B. Ling, J.L. Zhao, Z.L. Dong, Electroluminescence from ferromagnetic Fe doped ZnO nanorod arrays on P–Si. *IEEE Trans. Electron. Device* **57**, 1948–1951 (2010)
21. Y. Nam, I. Hwang, B.H. Park, Switchable Schottky diode characteristics induced by electroforming process in Mn doped ZnO thin films. *App. Phys. Lett.* **102**, 162105 (2013)
22. H. Emrah Unalan, P.H. Hiralal, M. Chhowalla, Flexible organic photovoltaics from Zinc oxide nanowires grown on transparent and conducting single walled carbon nanotube thin films. *J. Mater. Chem.* **18**, 5909–5912 (2008)
23. L. Zhifang, C. Guangyu, L. Liwei, Development of aluminium-doped ZnO films for a Si:h/μc-Si: H solar cell applications. *J. Semicond.* **34**, 063004 (2013)
24. X. Zhang, X. Huang, H. Jiang, Dye-Sensitized solar cell with energy storage function through PVDF-ZnO nanocomposite counter electrode. *Adv. Mater.* **25**, 4093–4096 (2013)
25. A. Kharatzadeh, F. Jamali-Sheini, R. Yousefi, Excellent photocatalytic performance of Zn(1–x)Mg<sub>x</sub>O/rGO nanocomposites under natural sunlight irradiation and their photovoltaic and UV detector applications. *Mater. Design* **107**, 47–55 (2016)
26. R.F. Dezfulya, R. Yousefi, F. Jamali-Sheini, Photocurrent applications of Zn(1–x)Cd<sub>x</sub>O/rGO nanocomposites. *Ceram. Int.* **42**, 7455–7461 (2016)
27. A. Saaedi, R. Yousefi, F. Jamali-Sheini, A.K. Zak, M. Cheraghizade, M.R. Mahmoudian, M.A. Baghchesara, A.S. Dezaki, XPS studies and photocurrent applications of alkali-metals-doped ZnO nanoparticles under visible illumination conditions. *Physica E* **79**, 113–118 (2016)
28. D. Sridevi, K.V. Rajendran, Synthesis and optical characteristics of ZnO nanocrystals. *Bull. Mater. Sci.* **32**, 165–168 (2002)
29. Dharma J, Pital A., Simple method of measuring the band gap energy value TiO<sub>2</sub> in powder form using a UV/Vis/NIR spectrometer, *Application Note*, PerkinElmer Inc
30. M. Elahi, D. Souri, Study of optical absorption and optical band gap determination of thin amorphous TeO<sub>2</sub>–V<sub>2</sub>O<sub>5</sub>–MoO<sub>3</sub> blown films. *J. Pure Appl. Phys.* **44**, 468–472 (2006)
31. K. Omar, M.D.J. Ooi, M.M. Hassin, Investigation on dielectric constant of Zinc oxide. *Mod. Appl. Sci.* **3**, 110 (2009)
32. S. Shah, D. Singh, V. Shrinet, Dielectric properties and surface morphology of proton irradiated ferric oxalate dispersed PVC films. *J. Pure Appl. Phys.* **46**, 439–442 (2008)
33. A. Roy, A. Parveen, A. Koppalkar, Microscopic and dielectric studies of ZnO nanoparticles loaded in ortho-chloropolyaniline-nanocomposites. *J. Nanopart. Res.* **15**, 3–11 (2013)